Electrohydraulic Crimping of 316L Tube in a 316L Thick Ring

R. Le Mentec[1-3*], C. Sow[2], T. Heuzé[1], G. Racineux[1]

[1] Institut de Recherche en Génie Civil et Mécanique, Ecole Centrale de Nantes, 1 rue de la Noë, 44321 Nantes cedex3, France
[2] IRT Jules Verne, Chemin du Chaffault, 44340 Bouguenais, France
[3] Naval Group, - Technocampus Océan - 5, rue de l'Halbrane 44340 Bouguenais
*Corresponding author. Email: Ronan.Le-Mentec-Guichon@ec-nantes.fr

Abstract

During the electrohydraulic forming process a high current, up to one hundred of kilo-amperes, is discharged between two electrodes immersed in a water tank. This creates plasma that generates a primary shock wave and secondary pressure waves. If these pressures are applied in a tube, it is then possible to deform dynamically this tube against a ring, leading to crimping. This process presents several advantages: it is possible to deform internally tubes of diameters ranging from a few millimetres to several centimetres, no lubrication is needed and because the process is dynamic, the spring back is limited and some materials can present an improved behaviour compared to quasi-static forming.
In this paper, we present an original electrohydraulic crimping device. We successively present the operating principle of our system, the time evolution of the crimping pressure and the strain rate in the tube for two kinds of pulse shaper. Finally crimping tests are done to evaluate the efficiency of the process.

Keywords

Electrohydraulic, Crimping, Shock waves, Secondary waves

1 Introduction

There are conventionally two types of crimping, crimping by positive clearance and crimping by negative clearance (Ken-ichiro Mori et al., 2013). In the case of crimping by

negative clearance, the outer and inner parts to be assembled, must be either force-fitted or fitted after heating the outer part and / or cooling the inner part. In the case of crimping by positive clearance, one of the two parts must be plastically deformed. Mechanical, hydraulic or magnetic pulse processes are conventionally used (Kumar & Kore, 2019). Koen et al have indeed shown that the magnetic pulse process is a very relevant process for making crimped assemblies with positive clearance (Faes et al., 2012). As it has been observed experimentally, high strain rate processes reduce springback (V. Psyk et al., 2010). This can, in the context of crimping, present a major advantage.

Unfortunately, when it comes to deforming a tube in a bore, if the tube is made of a material that is a poor conductor of electricity or if its diameter is too small, the magnetic pulse process cannot be used. As part of this study, we propose an alternative to the magnetic pulse process, by adapting the electro-hydraulic forming process in order to crimp, from the inside, a tube in a relatively small diameter bore.

The electro-hydraulic forming process consists of performing an electric arc in water (Laforest et al., 2018) (John J.F. Bonnen & Sergey F. Golovashchenko, 2013). The deposition of electrical energy, as heat energy, in a plasma generates pressure waves in water. A few microseconds after the discharge, we observe the appearance of a so-called primary shock wave and a few tens of microseconds later secondary pressure waves which result from the oscillation of a vapor bubble. To perform forming or crimping by electrohydraulic discharge, it is therefore sufficient to ensure that the pressure waves propagate towards the surfaces to be deformed. This process is widely used for sheet metal or tube forming operations. It has also been used to perform crimping when the diameter of the tube allows (Priem et al., 2007).

To achieve a crimp at the entrance of a small diameter tube, it is necessary to conduct the pressure waves inside the tube while maintaining the intensity and speed of the loading. Within the framework of this work we propose two configurations of electro-hydraulic crimping. For each of them we have qualified the loading that can be applied inside of a crimped tube and we have also carried out initial tests in order to assess the quality of the assemblies thus made. The results obtained are finally commented on.

2 Material and Methods

2.1 Materials

For this study, we used 316L stainless steel tubes and rings. ***Table 1*** shows the chemical composition of this alloy. At room temperature this material has a density of 7900 kg / m^3, a Young's modulus of 193 GPa and a Poisson's ratio of 0.3.

%C	%Mn	%P	%S	%Si	%Cr	%Ni	%Mo	%N	%O	%Fe
< 0.03	< 2	< 0.01	< 0,005	< 1	16-19	10.5-13	1.5-3	< 0.003	< 0.002	Compl

Table 1*: Chemical composition of stainless steel 316L*

The tubes have an outer diameter $D_e = 28$ mm, a thickness $e = 1.5$ mm and a length $L = 60$ mm. The rings have an outer diameter $D_{r_e} = 43$ mm, an inner diameter $D_{r_i} = 28$ mm and a length $L_r = 23$ mm.

2.2 Pulsed Current Generator

The pulse generator used is a 50 kJ, developed at Ecole Centrale Nantes with the following characteristics:

$$C_{Gen} = 408\ \mu\text{F};\ L_{Gen} = 0.1\ \mu\text{H};\ R_{Gen} = 3\ \text{m}\Omega;\ V_{max} = 15\ \text{kV};\ I_{max} = 500\ \text{kA}$$

with C_{Gen}, L_{Gen}, V_{max} denote respectively the capacity, the inductance and the maximum discharged current of the generator.

The highest limit for the discharge energy is hence fixed at 16 kJ so that the discharge current does not exceed 80% of the maximum allowable current for the generator:

$$I_{operation\ max} = 0.8 \times I_{max} = 400\ \text{kA}$$

2.3 Crimping System

In this study, we developed an original electrohydraulic crimping system. This system is made up of three subsystems (**Fig. 1**): (1-2) an electro-hydraulic waves generator which generates high amplitude pressure waves in water; (3a – 3b) a pulse shaper and (4) a crimping probe including openings, which is placed in the tube to be crimped. Depending on the desired crimping conditions (strain rate), we designed two pulse shapers to conduct and amplify pressure waves. An acoustic pulse shaper allows amplifying the primary shock wave while a mechanical pulse shaper allows filtering the shock wave and amplifying the secondary waves.

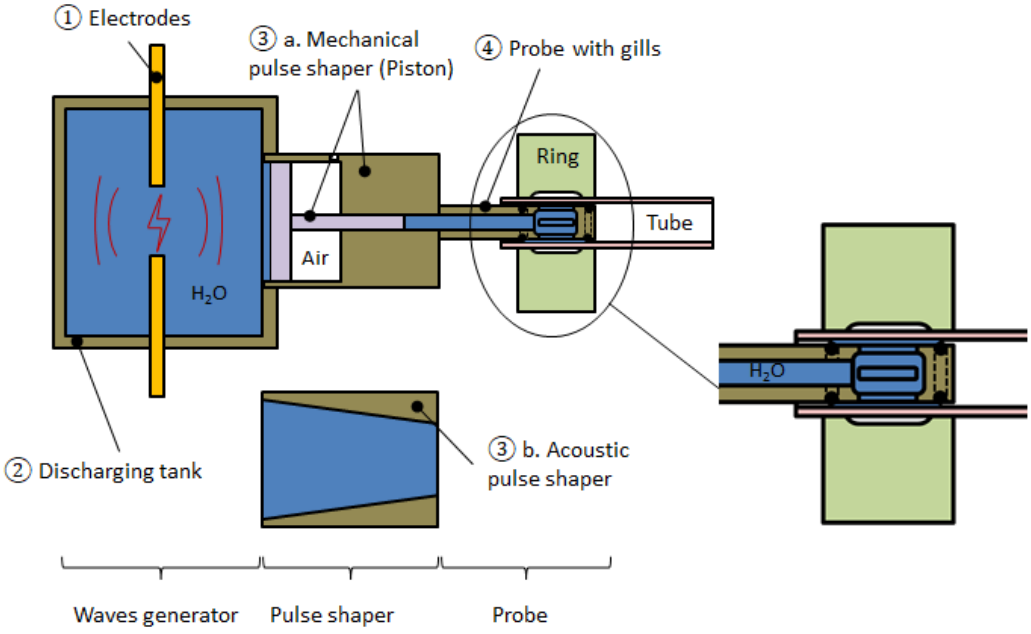

Figure 1: *Electrohydraulic crimping system*

2.4 Current and Pressure Measurement

To measure the discharge current, we used a Rogowski coil CWT1500 from PEM (Power Electronic Measurements). To measure the pressure, we used a quartz sensor marketed by the Kistler company (model 6213B). This sensor has a measurement range from 0 to 10,000 bars. The bandwidth is 150 kHz.

2.5 Pullout Force Measurement

To assess the quality of the crimps between the ring and the tube, we used the device shown in **Fig. 2**. The crimped tube and ring are placed in a cylinder, resting on an internal shoulder. A piston whose end fits into the tube, allows to apply a force to the tube. The entire assembly is positioned in a compression testing machine. The maximum pullout force F_{max} corresponds to the force F reached at the slip limit. If the residual contact pressure p_{cr} is homogeneous on the contact surface, then:

$$p_{cr} = \frac{F_{max}}{\mu \pi D_{r_i} L_r} \quad (1)$$

where μ, D_{r_i} and L_r denote respectively the friction coefficient between the ring and the tube, assumed equal to 0.3 in this study, the inner diameter and the length of the ring.

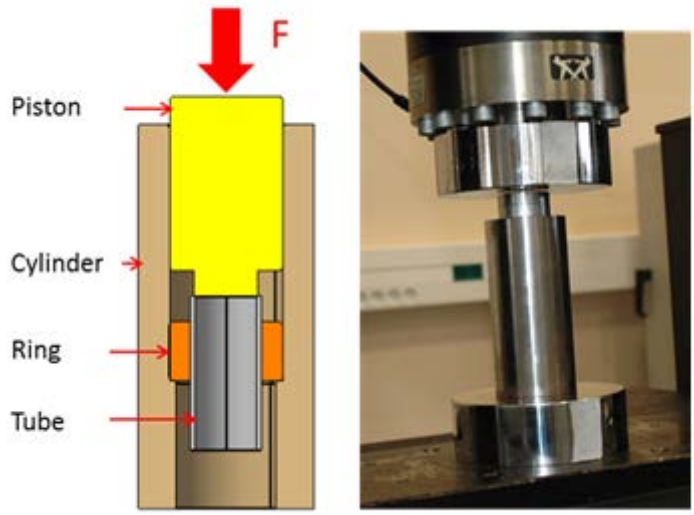

Figure 2 : *Device for measuring the pullout force*

2.6 Device to Measure the Crimping Pressure

Fig. 3 shows the device used to measure the pressure applied by the probe at the output of the pulse shapers. A thick ring, supposedly rigid, is fitted onto the probe. The pressure sensor is attached to the ring in the radial direction.

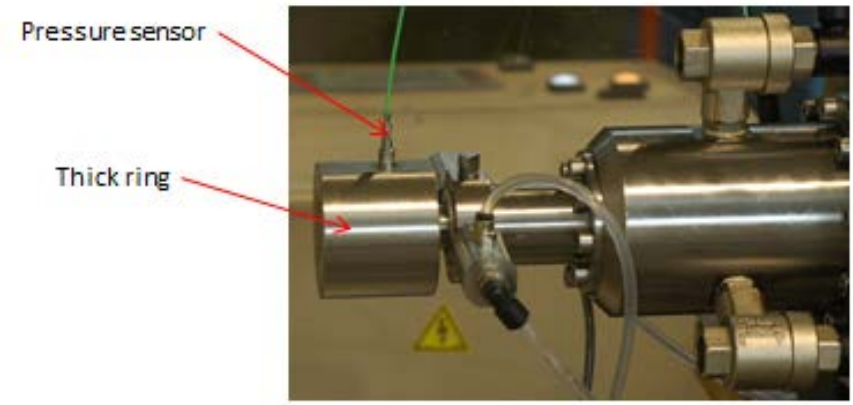

Figure 3 : *Device for measuring the pressure at the probe outlet*

2.7 Device to Measure the Strain Rate in the Tube

Fig. 4 shows the setup used to measure the tube strain rate. The tube is fitted onto the probe. Two rigid retaining rings help to block the deformation of the tube above the probe seals. The tube is free to expand between the rings. In order to measure the displacement of a point on the periphery of the tube during free expansion, we used a high-speed Photron SA1 camera. Its acquisition speed varies between 5,400 images per second for a resolution of 1024 x 1024 pixels and 675,000 images per second for a resolution of 64x16 pixels. We chose a resolution of 256x128 pixels, which allowed us to have an acquisition speed of 125,000 images per second, or one image every 8 microseconds.

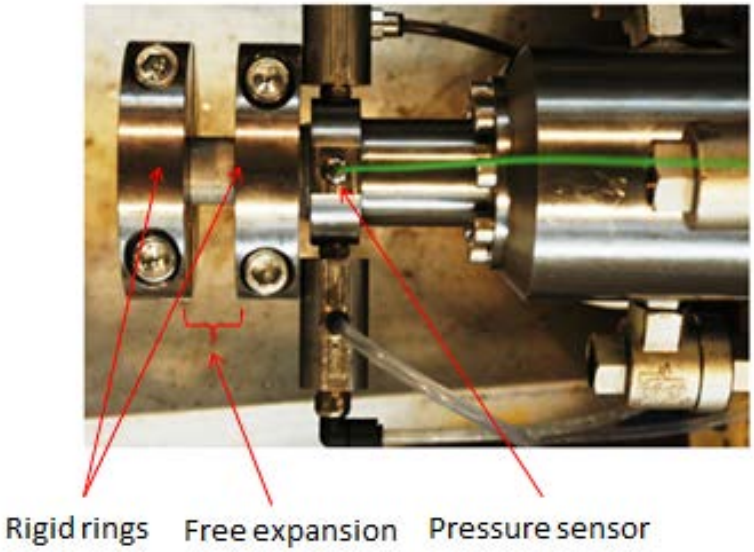

Figure 4 : *Device for measuring the strain rate*

3 Results and discussion

3.1 Pressure measurement

Fig. 5 shows the evolution of the pressure signal, measured at the output of the probe during a test at 8 kJ for an inter-electrode distance of 2.5 mm using the device shown in **Fig. 3** with the acoustic pulse shaper. This signal is characteristic of a confined electro-hydraulic discharge. A shock wave is observed first and then secondary waves. The shock wave, with an amplitude of 3200 bars, arrives around 300 µs after the start of the discharge at the measuring point, while the first secondary wave, with amplitude of less than 300 bars, arrives 2000 µs after the start of the discharge at the measuring point. These secondary waves result from the oscillations of the vapor bubble (Gilles Touya, 2003).

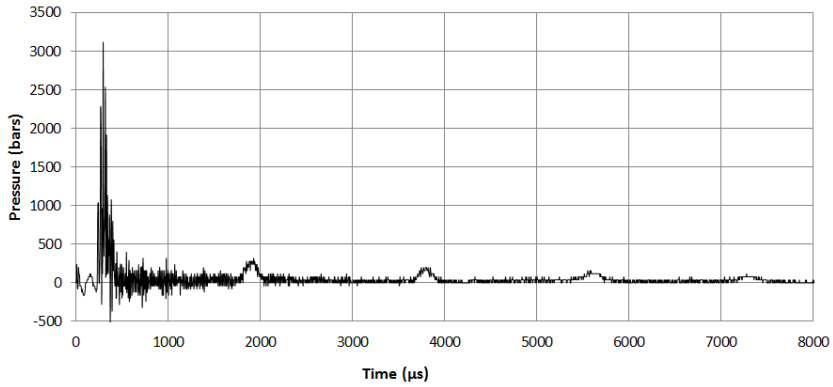

Figure 5 : *Pressure signal with acoustic pulse shaper*

Fig. 6 shows the evolution of the pressure signal, measured at the output of the probe during a test at 8 kJ for an inter-electrode distance of 2.5 mm using the device shown in **Fig. 3** with the mechanical pulse shaper. We do not observe a shock wave but only what appears to be an image of the secondary waves emitted by the wave generator. The first pressure wave arrives at the measuring point 760 µs after the start of discharge and has an amplitude of 1680 bars. The mechanical pulse shaper therefore acts as a low pass filter.

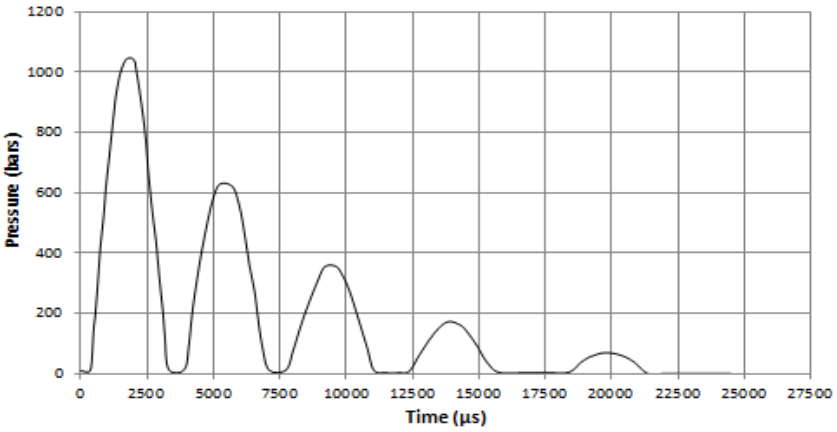

Figure 6 : *Pressure signal with mechanical pulse shaper*

3.2 Strain rate measurement

In order to evaluate the strain rate reached with the electro-hydraulic forming / crimping system, we carried out a free expansion test, with an energy of 8kJ and an inter-electrode distance of 2.5 mm by using the device shown in **Fig. 4**. With the high speed camera, we measured the evolution over time of the outer diameter D_e of the tube (**Fig. 7**). It was therefore possible to deduce the temporal evolution of the maximum orthoradial deformation:

$$\epsilon_\theta = \ln(1 + \frac{D_e}{D_{e_0}}) \quad (2)$$

and therefore, the strain rate. The measured strain rate is about 10^3 s^{-1} with the acoustic pulse shaper and 10^2 s^{-1} with the mechanical pulse shaper.

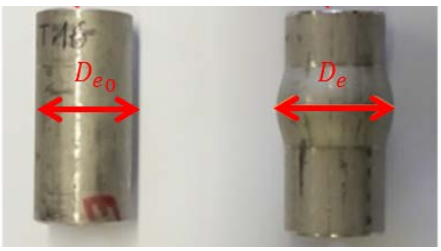

Figure 7 : *Tube before and after free expansion*

3.3 Crimping experiments

In order to evaluate the efficiency of the electro-hydraulic tube crimping process, we carried out tests for an energy varying from 6 kJ to 16 kJ and a launch clearance (clearance between the outer radius of the tube and the inner radius of the ring) of 0.1 mm, 0.2 mm and 0.3 mm. Each test was repeated a minimum of three times. It should be noted that with the acoustic pulse shaper (APS), regardless of the launch clearance, it was not possible to crimp the tube for an energy less than 16 kJ. Likewise, with the mechanical pulse shaper, it was not possible to crimp below 8 kJ.

Fig. 8 shows the evolution of the maximum pullout force (F_{max}) as a function of the pressure measured (p) during crimping experiments (the peak pressure of the first wave). To measure these forces, we used the device shown in **Fig. 2**. Several observations can be made:

- With the acoustic pulse shaper, the measured pullout force is less than 1000 N and no tendency can be observed regarding the launching clearance;
- With the mechanical pulse shaper (MPS), for pressures lower than those applied with the acoustic pulse shaper, we measure maximum pullout forces up to 7370 N. This seems to demonstrate that the intensity of the pressure wave is not sufficient to achieve a crimp. The load must be applied for a sufficiently long time. The mechanical pulse shaper, which uses secondary waves rather than the primary shock wave, is therefore logically more efficient;

- With the mechanical pulse shaper, it can be noticed that the smaller the launching clearance is, the better the crimp is. In order to qualify these assemblies and assess the potential of this technology (reduction of elastic return at high strain rate), it will be necessary to compare these results with those obtained by quasi-static hydraulic crimping.

For a better understanding of the difficulties observed with the acoustic pulse shaper, it will be necessary to carry out numerical simulations. In fact, it is likely that a rebound of the tube in the ring will take place in this configuration. This is all the more likely that the tube and the ring have the same acoustic impedances (Sow et al., 2020). Moreover, it should be noted that the fact of having chosen identical materials for the tube and the ring is the worst case from a crimping point of view (Maxwell, 1943).

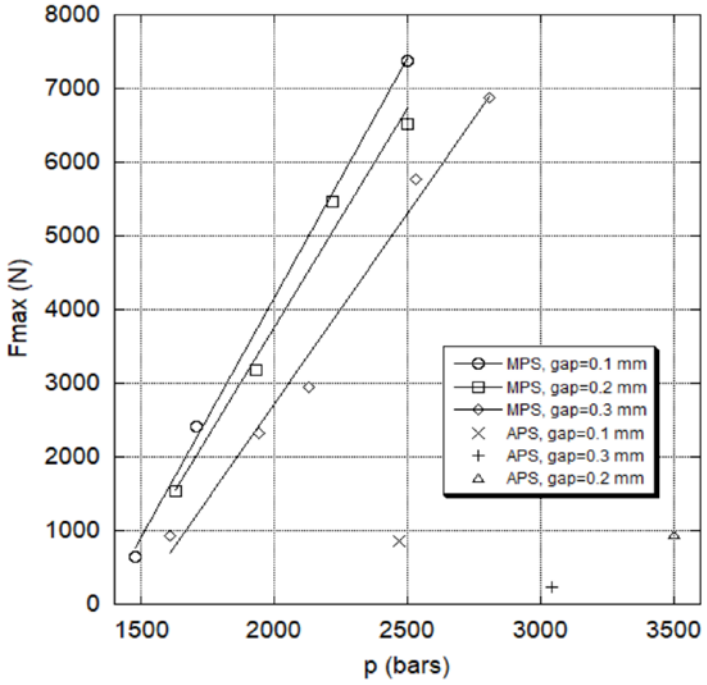

Figure 8 : *Evolution of pullout force as a function of measured pressure*

4 Conclusions

In this study, we propose an original way to crimp a tube at high strain rate in a ring by electrohydraulic discharge. In order to exploit either the primary shock wave or the secondary waves, two systems are proposed. These systems, called pulse shaper, work to amplify the pressure waves and guide them inside the crimp tube. The work carried out shows that the strain rates are in the order of 10^2 s^{-1} with the mechanical pulse shaper (MPS) and 10^3 s^{-1} with the acoustic pulse shaper (APS). Crimping tests have demonstrated the ability of the crimping process with MPS to join small dimension 316L tubes into rings of the same material. The use of APS does not allow assembly. Complementary work must be carried out to compare the quality of assemblies produced dynamically compared to

quasi-static hydraulic crimps. Numerical simulations of process with APS should provide a better understanding of the dynamic effects that are likely to be the cause of poor system performance.

5 Acknowledgments

This study is part of the HPP project managed by IRT Jules Verne (French Institute in Research and Technology in advanced manufacturing Technologies for composite, metallic and hybrid structures). The authors wish to acknowledge the industrial and academic partners of the project: *Airbus*, *Airbus Group Innovations*, *Constellium*, *Europe Technologies*, *Stelia Aerospace* and *Ecole Centrale de Nantes* respectively.

References

Faes, K., Zaitov, O., & De Waele, W. (2012). Electromagnetic pulse crimping of axial form fit joints. *Proceedings of the 5th International Conference on High Speed Forming*, 229–242.

Gilles Touya. (2003). *Contribution a l'etude experimentale des decharges electriques dans l'eau et des ondes de pression associees*. Universite de Pau et des Pays de l Adour.

John J.F. Bonnen, & Sergey F. Golovashchenko. (2013). Electrode {Erosion} {Observed} in {Electrohydraulic} {Discharges} {Used} in {Pulsed} {Sheet} {Metal} {Forming}. *Journal of Materials Engineering and Performance*.

Ken-ichiro Mori, Niels Bay, Livan Fratini, Fabrizio Micari, & A. Erman Tekkaya. (2013). Joining by plastic deformation. *CIRP Annals - Manufacturing Technology*.

Kumar, R., & Kore, S. D. (2019). Experimental Studies on the Effect of Different Field Shaper Geometries on Magnetic Pulse Crimping in Cylindrical Configuration. *The International Journal of Advanced Manufacturing Technology*, *105*(11), 4677–4690.

Laforest, Z., Gonzalez, J.-J., & Freton, P. (2018). Experimental study of a plasma bubble created by a wire explosion in water. *IJRRAS*, *34*.

Maxwell, C. A. (1943). Practical aspects of making expanded joints. *Trans. ASME*, *65*, 506–522.

Priem, D., Marya, S., & Racineux, G. (2007). On the forming of metallic parts through electromagnetic and electrohydraulic processing. *Advanced Materials Research*, *15*, 655–660.

Sow, C. T., Bazin, G., Heuzé, T., & Racineux, G. (2020). Electromagnetic flanging: from elementary geometries to aeronautical components. *International Journal of Material Forming*, *13*(3), 423–443.

V. Psyk, D. Risch, B.L. Kinsey, A.E. Tekkaya, & M. Kleiner. (2010). Electromagnetic forming—(A) review. *Journal of Materials Processing Technology*.